

Characterization of Inhibitors for Cu/Zn
Superoxide Dismutase Observed by ^{19}F NMR
Methods

A thesis presented to the faculty of the Graduate School
of Western Carolina University in partial fulfillment of the
requirements for the degree of Master of Science in
Chemistry

By

Jonathan Markley

Research Advisor: Dr. Jack Summers

Associate Professor

Chemistry Department

Committee Members: Dr. Brian Dinkelmeyer, Chemistry
Dr. Chris Coburn, Biology

April, 2010

ACKNOWLEDGEMENTS

First and foremost I would like to thank my research committee Chris Coburn, Brian Dinkelmeyer and Jack Summers for their advice, support, guidance, expertise and patience throughout my research. With their support I have acquired the skills and methods necessary to complete the goals that I have set for myself. I would also like to thank the entire Chemistry and Physics department for their words of encouragement, humor and support throughout my graduate career. Last but not least I must thank my family who have molded me into the man and father that I am now.

I dedicate this work and my future endeavors to my daughter and son who have driven me to overcome the obstacles that have been placed in my path. My success in my field and beyond is a manifestation of their unconditional love and the joy that they bring their father.

Table of Contents

LIST OF TABLES.....	4
LIST OF FIGURES.....	5
LIST OF ABBREVIATIONS.....	6
ABSTRACT.....	7
1. INTRODUCTION.....	9
2. EXPERIMENTAL.....	12
2.A.1 FLUORIDE RELAXATION ENHANCEMENT BY SOD.....	12
2.A.2 ¹⁹ F NMR METHODS.....	12
2.B.1. STANDARDIZED CU/ZN SAMPLES.....	14
2.B.2. FLAVONOID SAMPLES.....	14
2.B.3 FLUORIDE BUFFER SAMPLES.....	15
2.C. DDC REACTION RATE.....	15
2.D. ENMD-1198 & 2-ME INHIBITOR SCREENING.....	16
2.E. GLYOXAL INHIBITION OF CU/ZN-SOD.....	16
2.F. MDHB INHIBITION.....	17
2.G. QUERCITIN MECHANISM OF INHIBITION.....	17
2.H. PH DEPENDANT QUERCITIN INHIBITION OF Cu/Zn-SOD.....	18
2.I.1 DISSOCIATION CONSTANTS FOR FLAVONOID INHIBITORS OF SOD.....	18
2.I.2 EMISSION SPECTRA FOR FLAVONOID INHIBITORS.....	19
3. RESULTS AND DISCUSSION.....	20
3.A. DDC RATE CONSTANT AND APPARENT REACTION ORDER.....	20
3.B. 2-ME, ENMD-1198 & GLYOXAL INHIBITOR SCREENING.....	22
3.C. MDHB INHIBITION.....	23
3.D. QUERCITIN MECHANISM OF INHIBITION.....	24
3.E. PH DEPENDANT QUERCITIN INHIBITION OF Cu/Zn-SOD.....	26
3.F.1 DISSOCIATION CONSTANTS FOR FLAVONOID INHIBITORS OF SOD.....	31
3.F.2 DIMERIZATION OF FLAVONOID INHIBITORS.....	38
4. CONCLUSIONS.....	42
REFERENCES.....	44

LIST OF TABLES

Table 1: Buffer pKas for fluoride buffer solutions.....	14
Table 2: Flavonoid pKas	19
Table 3: Initial Inhibition of SOD by glyoxal in pH 10 fluoride buffer soln.	23
Table 4: Calculated Cu/Zn-SOD inhibitor K_d and K_{dimer}	31

LIST OF FIGURES

Figure 1: Chemical structure of quercetin	10
Figure 2: k_{app} for DDC inhibition of SOD in pH 7 phosphate buffer	22
Figure 3: Reaction order for DDC in pH 7 phosphate buffer	22
Figure 4: MDHB inhibition of SOD in pH 10 glycine buffer	24
Figure 5: R_2 of fluoride in $CuSO_4$ quercetin and SOD dissolved in pH 10 buffer.....	25
Figure 6: Inhibition of Cu/Zn-SOD by 50 μ M quercetin in pH 6.16 citrate buffer	27
Figure 7: Inhibition of Cu/Zn-SOD by 50 μ M quercetin in pH 7.01 HEPES buffer.....	27
Figure 8: Inhibition of Cu/Zn-SOD by 50 μ M quercetin in pH 7.3 HEPES buffer.....	28
Figure 9: Inhibition of Cu/Zn-SOD by 50 μ M quercetin in pH 8.0 TRIS buffer.....	28
Figure 10: Inhibition of Cu/Zn-SOD by 50 μ M quercetin in pH 8.5 TRIS buffer.....	29
Figure 11: Inhibition of Cu/Zn-SOD by 50 μ M quercetin in pH 9 glycine buffer.....	29
Figure 12: Inhibition of Cu/Zn-SOD by 50 μ M quercetin in pH 9.5 glycine buffer.....	30
Figure 13: Inhibition of Cu/Zn-SOD by 50 μ M quercetin in pH 10 glycine buffer.....	30
Figure 14: Inhibition of Cu/Zn-SOD by 50 μ M quercetin in pH 10.5 glycine buffer.....	31
Figure 15: Inhibition of Cu/Zn-SOD by morin dissolved in pH 8.01 TRIS buffer.....	34
Figure 16: Inhibition of Cu/Zn-SOD by luteolin dissolved in pH 8.01 TRIS buffer	34
Figure 17: Inhibition of Cu/Zn-SOD by taxifolin dissolved in pH 8.01 TRIS buffer	35
Figure 18: Inhibition of Cu/Zn-SOD by methoxyquercetin in pH 8.01 TRIS buffer	35
Figure 19: Inhibition of Cu/Zn-SOD by kaempferol in pH 8.01 TRIS buffer.....	36
Figure 20: Inhibition of Cu/Zn-SOD by fisetin in pH 8.01 TRIS buffer	36
Figure 21: Inhibition of Cu/Zn-SOD by quercetin in pH 8.01 TRIS buffer.....	37
Figure 22: Excitation spectra for taxifolin dissolved in pH 8.01 fluoride TRIS soln.....	39
Figure 23: Excitation spectra for fisetin dissolved in pH 8.01 fluoride TRIS soln.....	40
Figure 24: Excitation spectra for morin dissolved in pH 8.01 fluoride TRIS soln.....	40
Figure 25: Excitation spectra for kaempferol dissolved in pH 8.01 fluoride TRIS soln.....	41
Figure 26: Excitation spectra for quercetin dissolved in pH 8.01 fluoride TRIS soln.....	41

LIST OF ABBREVIATIONS

k_{app}	apparent rate constant
k_{obs}	observed rate constant
K_d	dissociation constant
K_{dimer}	dimerization constant
O_2^-	superoxide
SOD	superoxide dismutase
R_2	transverse relaxation rate
2-ME	2-methoxyestradiol
MDHB	methyl,3,4-dihydroxybenzoate
DDC	diethyldithiocarbamate
$Inh_{monomer}$	calculated concentration of inhibitor
Inh	free inhibitor
SOD_{Active}	fraction of SOD active
$SOD_{Inactive}$	fraction of SOD inactive
NMR	nuclear magnetic resonance
tfa	trifluoroacetate
I_{obs}	integrated fluoride signal
I_0	initial integrated fluoride signal
cpmg	Carr-Purcell-Meiboom-Gill
I_F	integrated fluoride signal
I_{tfa}	integrated trifluoroacetate signal
DMSO	dimethylsulfoxide
Cu/Zn-SOD	copper zinc superoxide dismutase
Fe-SOD	Iron superoxide dismutase
A_0	Initial fraction of SOD activity

ABSTRACT

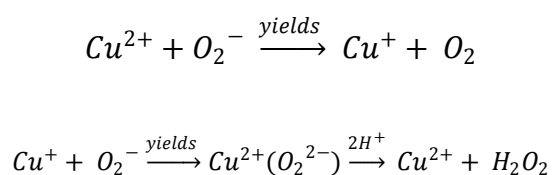
Superoxide dismutase (SOD) is an enzyme that disproportionates superoxide (O_2^-) into H_2O_2 and O_2 . The inhibition of this enzyme could be a novel method for the treatment of chronic diseases such as leukemia, cancer and malaria.^{2,7,8} Methods that rely on superoxide generating systems have been used previously to assay SOD activity and to search for inhibitors⁶. The reliability of these methods for screening inhibitors is limited due to the reactivity of superoxide as well as well as the indicators these methods used.⁷ Our group uses the more stable fluoride anion as an indicator of SOD activity. ^{19}F NMR techniques that measure the rate at which fluoride relaxes (R_2) were used to assay inhibitors for Cu/Zn-SOD. Inhibitors we studied included 2-methoxyestradiol (2-ME), glyoxal, flavonoids, methyl-3,4-dihydroxybenzoate (MDHB) and diethyldithiocarbamate (DDC). We have measured the kinetics of SOD inhibition as a function of DDC concentration. We have DDC inhibition of SOD to first order with an apparent rate constant of 0.0125 s^{-1} . Our experiments indicate that quercetin does not inhibit SOD by sequestering the copper ion from enzyme active site. The effects of the flavonoids quercetin, luteolin, morin, fisitin, kaempferol, taxifolin and methoxyquercetin on SOD activities were studied as a function of flavonoid concentration. Kinetic studies of SOD inhibition indicated a two step reaction where the first step was a rapid equilibrium. The effects of flavonoid concentration on the initial SOD activity (from kinetic plots) suggested that these compounds dimerize under the conditions of the experiment, and that dimerization competes with enzyme inhibition. The effects of flavonoid

concentrations on their luminescence spectra supported this hypothesis.

Inhibition and dimerization equilibrium constants were estimated by fitting the curves predicted by the dimerization model to the inhibition data.

1. INTRODUCTION

Superoxide (O_2^-) formation elicits oxidative stress that has been linked to various diseases.¹ The accumulation of O_2^- leads to mitochondrial membrane damage that triggers cell apoptosis.² Tissue samples subjected to oxidative stress from O_2^- have exhibited an increase in superoxide dismutase (SOD) concentrations. SOD is a dimeric enzyme that catalyzes the conversion of O_2^- into hydrogen peroxide and molecular oxygen. Fe-SOD is found in a number of parasitic protozoa and constitutes the primary enzymatic defense against O_2^- induced damage.³ Cu/Zn-SOD is found in most eukaryotes, few prokaryotes and is structurally different from the Fe-SOD species. Inhibitors for Fe-SOD have shown little effect on Cu/Zn-SOD.³ This observed inhibitor selectivity could be a great avenue to treat diseases such as leukemia, malaria and cancer, which rely on SOD to eliminate free radical accumulation.² Our research group has focused on the characterization of inhibitors for Cu/Zn-SOD. Cu/Zn-SOD eliminates O_2^- by the disproportionation reaction below.⁴



SOD has an extremely high turnover rate and is resistant to thermal and chemical denaturation. The enzyme is stable at 80°C and retains activity in 4%

sodium dodecyl sulfate and in 8M urea.⁴ Cu/Zn-SOD activity is unaffected by solution pH within the range of 5-10.⁴

Commonly used methods for observing SOD activity rely on the production of O_2^- .¹ Systems that rely on generation and detection of superoxide suffer from problems associated with the high reactivity of O_2^- . Produced O_2^- interacts with more than SOD and most likely is interfering with the O_2^- generating system as well as the indicator.⁷ Produced H_2O_2 from the SOD mediated disproportionation of O_2^- has been shown to inactivate SOD which further invalidates previous methods.^{6,5} This makes accurately assaying SOD activity and inhibition impossible by using these methods. Our group uses ^{19}F NMR in place of an O_2^- generating system. The fluoride ion is excited and relaxes at a certain rate back to its ground state. SOD causes the fluoride to relax at a much faster rate than it normally would. This change in the fluoride relaxation rate (R_2) allows us to measure SOD activity in a sample, which in turn allows the characterization of enzyme/inhibitor interactions.

Heikkila et. al. has shown that DDC inhibits Cu/Zn-SOD by removing the copper from the active site.⁶ The stoichiometry of this reaction requires that at least two DDC molecules coordinate the metal. Since DDC (and other small molecule chelating agents) inactivate SOD by removing, we feel it is important to determine whether other inhibitors the metal inhibit SOD by similar action. Based on the crystal structure, Soullère et al proposed that the active site Fe-SOD, would not be available to bulky chelators.⁷ Other studies cited by the Soullère

group have shown that desferrioxamine and bathophenanthroline do not chelate iron from Fe-SOD supporting their hypothesis.⁷ This group hypothesizes that inhibitors interact with the entrance or inside the channel of residues that attract electronegative superoxide like compounds.⁷

2-ME is an estrogen derivative that has been shown to be protective agent against tumor formation.⁸ Previous works have shown that 2-ME shows potent selective activity against leukemia cells.² MDHB and glyoxal were chosen as possible inhibitors because of the two hydroxyl groups that could possibly attach at the SOD active site or channel. Quercetin (shown in Figure.1) is a naturally occurring flavonol that is found in many fruits, vegetables, teas and grapes. Quercetin is known for its antioxidant effects and some studies indicate that it may be beneficial in preventing prostate cancer.⁹

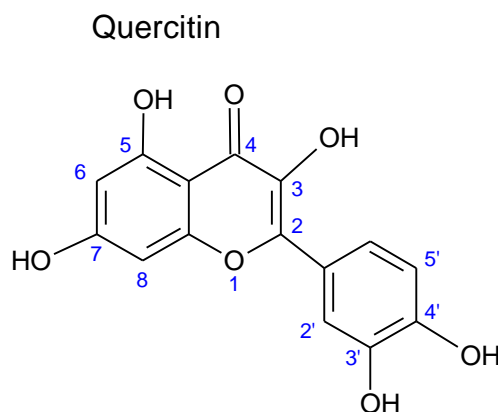


Figure 1: Chemical structure of quercetin

2. EXPERIMENTAL

2.A.1 FLUORIDE RELAXATION ENHANCEMENT BY SOD

The transverse relaxation (R_2) of fluoride can be observed using ^{19}F NMR methods. The R_2 of fluoride is increased in the presence of SOD due to coordination of the anion and the enzyme's metal active site. The amount by which the R_2 of fluoride increases has been shown to be proportional to the concentration of SOD.⁵ This allowed our group to quantify the SOD activities in our samples. A JEOL Eclipse 300 MHz NMR spectrometer was used for all fluoride relaxation experiments. Fluoride resonance peaks were obtained and then integrated using the Origin program. Fluoride, SOD, buffer solutions were placed in a constant water bath of 25°C for 30 minutes prior to measurements.

2.A.2 ^{19}F NMR METHODS

Transverse relaxation rates (R_2) of fluoride were measured by one of two methods. For inhibitor screening, we used a one-dimensional method that employs trifluoroacetate (tfa) as an internal reference. For quantitative work, we used the Carr-Purcell-Meiboom-Gill (*cpmg*) method. (Equation.1) was used to calculate observed R_2 values. The Integrated fluoride signal (I_{obs}) and the integrated signal at time 0 (I_0) were both observed values with (t) being the delay interval.

$$I_{\text{obs}} = I_0 e^{-R_2 t} \quad (1)$$

The equation was simplified further by taking the natural log of both sides and plotting $(\ln(I_{obs}) - \ln(I_0))$ vs. *delay interval* (t) giving a linear relationship with the slope being equal to $-R_2$.

The increase in the rate fluoride relaxes in the presence of enzyme has been observed by Rigo et al. to be dependent upon the [SOD].⁵ Using positive controls ($R_{2,SODControl}$) and negative controls ($R_{2,NegControl}$) the effect of inhibitor upon the fraction of SOD activity (SOD_{Active}) can then be calculated using the equation.

$$SOD_{Active} = \frac{R_{2,Sample} - R_{2,NegControl}}{R_{2,SODControl} - R_{2,NegControl}} \quad (2)$$

For experiments containing ENMD-1198, 2-ME, glyoxal and MDHB we used the 1D method employing trifluoroacetate (tfa) as an internal reference. Another member of our group has shown that the resonance integral of tfa is relatively un-changed by SOD.¹⁰ Using the integrated tfa resonance signal (I_{tfa}) and the integrated fluoride resonance (I_F) our group calculated the fraction of SOD activity (SOD_{Active}) by the equation.

$$SOD_{Active} = \frac{\left(\frac{I_{tfa}}{I_F}\right)_{Sample} - \left(\frac{I_{tfa}}{I_F}\right)_{NegControl}}{\left(\frac{I_{tfa}}{I_F}\right)_{SODcontrol} - \left(\frac{I_{tfa}}{I_F}\right)_{NegControl}} \quad (3)$$

2.B.1. STANDARDIZED CU/ZN SAMPLES

Bovine Cu/Zn-SOD was purchased from MP Biomedicals LLC. The enzyme was diluted to 1mL with HPLC grade water. 2 μ L was then removed and added to 588 μ L of 20mM fluoride buffer. The R_2 value for this sample was then determined using the cpmg method for the ^{19}F NMR. The concentration of enzyme for this sample was then adjusted to give an appropriate R_2 value between 30 sec^{-1} and 100 sec^{-1} . The remainder of the 1mL enzyme sample was divided into separate 1mL eppendorff tubes containing the same amount of enzyme as the adjusted sample. Each enzyme aliquot contained \sim 3000 units. These aliquots were then dehydrated using centrifugal evaporation and stored at -20°C . Before each experiment requiring enzyme the desiccated aliquots were removed from storage and rehydrated in 200 μ L of HPLC grade H_2O . Each rehydrated SOD eppendorff contained enough enzyme for 10 assay samples with each assay sample containing 20 μ L of rehydrated SOD.

2.B.2. FLAVONOID SAMPLES

Inhibitors were serially diluted in dimethylsulfoxide (DMSO) due to their low solubility in aqueous solutions. Flavonoid samples observed by ^{19}F NMR methods contained 12 μ L of morin, kaempferol, quercetin, luteolin, taxifolin, fisitin, methoxyquercetin, galangin or 3,3-dihydroxyflavone dissolved in 588 μ L of fluoride buffer solution. The solutions were vortexed for approximately 10 seconds after the addition of flavonoids to ensure proper mixture. The overall amount of DMSO present in any sample observed by ^{19}F NMR was 2% by volume.

2.B.3 FLUORIDE BUFFER SAMPLES

The fluoride buffer solution contained dissolved sodium fluoride (NaF) and buffer in HPLC grade water. Buffer solutions contained 20mM fluoride and 20mM buffer. The concentration of fluoride was therefore in great excess (10^{-1} M) compared to the concentration of SOD (10^{-7} M). Solution buffers were chosen according to their pKa's using the table of buffer pKa values below.

Buffer	pKa
PIPES	6.8
HEPES	7.55
Phosphate (PK ₂)	7.21
TRIS	8.3
Glycine	9.6

Fluoride buffer solutions used for ^{19}F NMR observations varied in alkalinity from pH 6 to pH 10.5. Fluoride buffer solutions contained 10% deuterium oxide (D_2O) by volume. Each fluoride buffer solution was adjusted to the desired pH by adding 1M KOH or 1M HCL.

2.C. DDC REACTION RATE

Our group observed the apparent rate (k_{app}) of Cu/Zn-SOD inhibition by DDC. The time between observations of fluoride resonance signals were minimized for the first hour to two hours to ensure that the change in R_2 was accurately represented. DDC samples contained pH 7 fluoride, SOD and phosphate buffer. Serially diluted DDC was added prior to observations to give concentrations of 2mM, 1mM, 0.5mM and 0.25mM. Professor Jack Summers

observed time dependent R_2 values for 1mM and 0.5mM DDC. Mickey Yost observed time dependent R_2 values for 2mM DDC. Jonathan Markley recorded time dependent R_2 values for 0.25mM DDC.

2.D. ENMD-1198 & 2-ME INHIBITOR SCREENING

Our group measured the fraction of SOD activity in the presence of ENMD-1198 and 2-ME. Both ENMD-1198 and 2-ME solutions were observed for a maximum of 3 days. ENMD-1198 and 2-ME were obtained from EntreMed Inc. Both sets of inhibitor samples contained pH 10.33 fluoride, tfa, glycine and SOD solution. ENMD-1198 and 2-ME were added prior to observations to give concentrations up to 100 μ M. Both tfa and fluoride resonance peaks were integrated using the ORIGIN program. The fraction of SOD active was calculated using (Equation.3).

2.E. GLYOXAL INHIBITION OF CU/ZN-SOD

Our group measured the fraction of SOD activity in the presence of glyoxal. Glyoxal containing enzyme samples were observed initially and 1 day later to observe any change in the fraction of SOD active. 8.8M glyoxal was obtained from the lab of Dr. William Kwotchka. Glyoxal samples were dissolved in pH 10.1 fluoride, SOD, glycine solution. Serially diluted glyoxal was added to fluoride buffer solution to give final inhibitor concentrations of 25mM, 5mM, 1mM and 250 μ M. The change in fluoride resonance (R_2) was observed by the cpmg method for ^{19}F NMR and integrated using the ORIGIN program. Observed

fluoride resonance was used to calculate R_2 values by (Equation.1). R_2 values were then used to calculate the fraction of SOD activity using (Equation.2).

2.F. MDHB INHIBITION

Our group observed the change in the fraction of SOD activity by the presence of MDHB as a function of time. The time between observations of tfa and fluoride resonance signals was minimized for the first two hours to ensure that the change in the fraction of SOD activity was accurately represented. Samples containing MDHB were dissolved in pH 10.33 fluoride, SOD, tfa and glycine buffer solution. Final sample inhibitor concentrations were 50 μ M, 1.25 μ M, 10mM and 20mM MDHB. Both tfa and fluoride resonance peaks were integrated using the ORIGIN program. The effect of MDHB on the fraction of SOD activity was calculated using (Equation.3).

2.G. QUERCETIN MECHANISM OF INHIBITION

The effect of Cu^{2+} on quercetin's ability to inhibit Cu/Zn-SOD was observed using WCU's NMR spectrometer. The R_2 values for all solutions were observed sequentially until there was no change in the observed R_2 . Observed samples contained CuSO_4 , $\text{CuSO}_4 + \text{SOD}$, quercetin + SOD and $\text{CuSO}_4 + \text{quercetin}$. Quercetin and CuSO_4 samples were dissolved in pH 10 fluoride, SOD, glycine solution. Free copper solutions contained 200 μ M CuSO_4 . Solutions containing dissolved quercetin had final concentrations of 50 μ M. Fluoride resonance peaks for all samples were observed by the cpmg method for ^{19}F

NMR and integrated using the ORIGIN program. Observed solution fluoride resonance was then used to calculate R_2 values by (Equation.1).

2.H. PH DEPENDANT QUERCETIN INHIBITION OF Cu/Zn-SOD

The change in the fraction of SOD activity was observed for solutions at different alkalinities and plotted as a function of time. Observed samples contained 50 μ M quercetin dissolved in fluoride, SOD buffer solution. Fluoride buffers were made with adjusted pH's being 6.5, 7, 7.3, 8, 8.5, 9, 9.5, 10 and 10.5. Observed fluoride resonance was used to calculate R_2 values by (Equation.1). Positive and negative controls allowed the quantification of the fraction of SOD active using (Equation.2)

2.1.1 DISSOCIATION CONSTANTS FOR FLAVONOID INHIBITORS OF SOD

Our group observed the effect of flavonoid concentration on the initial fraction of SOD activity (A_0). Observations of the A_0 were begun 2 minutes after the addition of inhibitor to enzyme containing solutions. Morin, quercetin, taxifolin, fisitin, luteolin, kaempferol, galangin, 3,3-dihydroxyflavone and methoxyquercetin were dissolved in pH 8.01 fluoride, TRIS buffer. Observed flavonoids were diluted to give final concentrations within the range of 6.25 μ M - 400 μ M. Concentrations of flavonoids below 6.25 μ M showed no observable change in the observed R_2 compared to the positive control. White precipitate was observed for flavonoid samples at or above 400 μ M. The pH of all solutions used for initial activity observations were 8.01 because the majority of inhibitors should be in their singly deprotonated species according to the table below.

Table 2: Flavonoid pKa's	
Flavonoid	pKa
quercetin	7.10, 9.09, 11.12 ¹²
morin	5.2, 8.2, 9.9 ¹¹
fisitin	7.27, 9.44 ¹²
kaempferol	6.96, 8.78, 10.60 ¹²

Fluoride resonance peaks of all flavonoids were observed by the cpmg method for ¹⁹F NMR and integrated using the ORIGIN program. The integrated fluoride resonance was used to calculate observed R₂ values by (Equation.1). Positive and negative controls allowed the quantification of the fraction of initial SOD active using (Equation.2).

2.1.2 EMISSION SPECTRA FOR FLAVONOID INHIBITORS

Our group observed excitation and emission spectra for morin, quercetin, taxifolin, fisitin, luteolin and kaempferol using a PerkinElmer LS55 luminescence spectrometer. All inhibitor samples were made within a few hours of absorbance/fluorescence observations to ensure no change in the solution pH for all observations. Observations were made at a path length of 1cm for all flavonoid samples. Excitation peaks were found experimentally by changing the emission scan wavelength until excitation peaks were maximized without loss of peak resolution. Emission slits were opened to 15mm and exit slits were set to 5mm which maximized observed peak heights without saturating the detector. Excitation spectra were observed within the ranges of 250nm to 460nm for all flavonoid samples. Fluorescence emission was observed within the ranges of

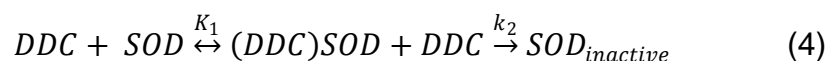
460 to 550nm. Observed flavonoid inhibitors were dissolved in pH 8.01 fluoride, TRIS buffer solution. Concentrations of flavonoids ranged from 400 μ M to 6.25 μ M. All observed samples contained the same 20mM F⁻, 20mM TRIS, pH 8.01 buffer.

3. RESULTS AND DISCUSSION

3.A. DDC RATE CONSTANT AND APPARENT REACTION ORDER

The mechanism of SOD inhibition by DDC has been hypothesized by our group to involve two molecules of DDC inhibiting one molecule of SOD. By our hypothesis the overall reaction order for DDC inhibition of SOD should be 2. Our results however indicate that the observed reaction order is 1 which suggests that our hypothesis on the mechanism of DDC inhibition is incorrect.

The first elementary step was hypothesized to be a quick one that involved one DDC molecule coordinating to the SOD active site and reaching equilibrium without sequestering the metal active site. The second elementary step then involved another DDC molecule coordinating with the DDC/SOD complex which then resulted in the sequestration of metal from the enzyme active site.



For our groups hypothesis the second elementary step was thought to be rate limiting so the rate of the overall inhibition of SOD by DDC should equal the second step rate constant (k_2) multiplied by [DDC] and the DDC/SOD complex [(DDC)SOD]. The apparent rate equation can be simplified into terms of [DDC], the first step's equilibrium constant (K_1), and the second elementary step's rate constant (k_2). The apparent rate can then be set equal to k_{app} which gives us the equation.

$$k_{app} = k_2 K_1 [DDC]^2 \quad (5)$$

In the presence of DDC, relaxation enhancement of the fluoride resonance decreased following pseudo-first order kinetics (Equation.6) Pseudo-first order rate constants for SOD inhibition (k_{obs}) were determined from the slopes of the kinetic plots (Figure 2).

$$R_{2,obs} = R_{2,neg} e^{-k_{obs} t} \quad (6)$$

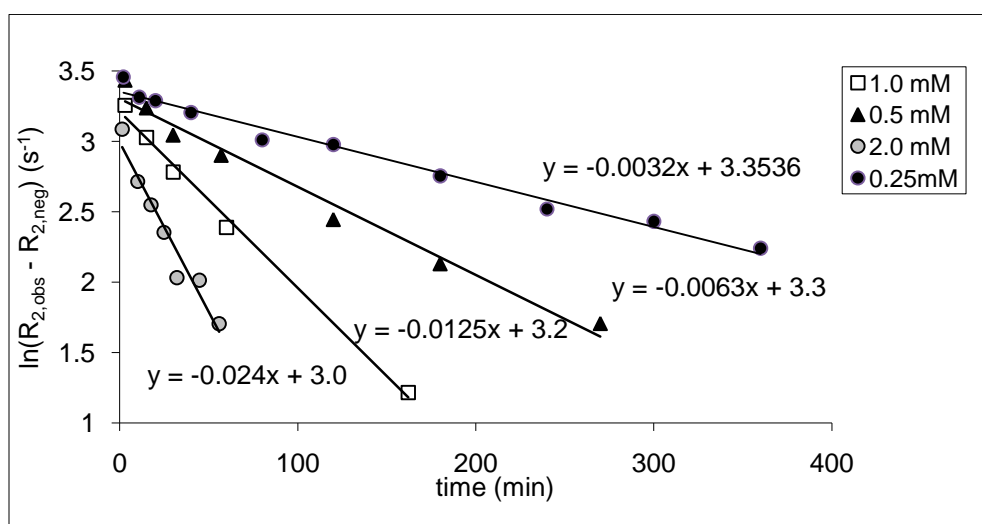


Figure 2: k_{app} for DDC inhibition of SOD in pH 7 phosphate buffer

Plotting the natural log of k_{obs} versus the natural log of [DDC] gave a linear plot with a slope of one (Figure 3).

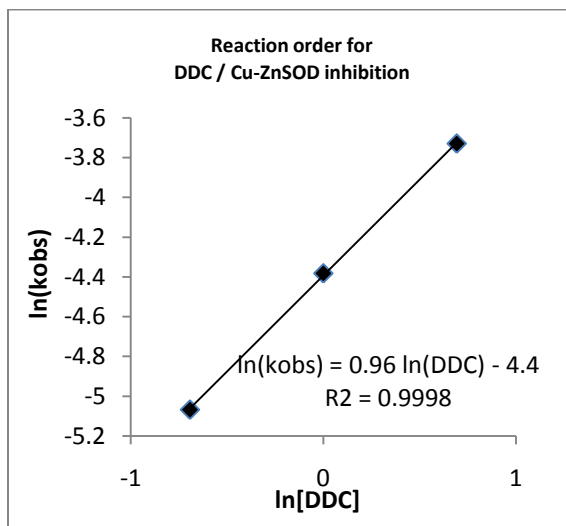


Figure 3: reaction order for DDC in pH 7 phosphate buffer

Thus, the data indicate that the rate at which DDC inhibits Cu/Zn-SOD is first order in DDC (Equation.7).

$$-d(\text{SOD})/dt = 8.1 \times 10^4 \text{ M}^{-1} \text{ s}^{-1} [\text{DDC}][\text{SOD}] \quad (7)$$

This result indicates that the reaction does not proceed via our hypothesized mechanism. This observed reaction order indicates that the first elementary step is rate limiting.

3.B. 2-ME, ENMD-1198 & GLYOXAL INHIBITOR SCREENING

2-ME has shown activity against leukemia cells with the hypothesis being that the cause of this observed activity was due to the inactivation of SOD within the leukemia cells.⁶ Our group tested this hypothesis by assaying 2-ME and another compound ENMD-1198. Addition of 2-ME and ENMD-1198 up to 100 μ M

showed no observable loss in SOD activity. This would suggest that no binding of SOD by either of these compounds occurred at or near the active site.

Our group assayed glyoxal to determine the effect the diketone functionality would have on SOD activity. Our observations indicate that the diketone does interact with the active site. A decrease in the fraction of SOD activity by glyoxal was observed within the ranges 250 μ M and 25mM. Near complete initial inhibition of SOD was observed for 25mM glyoxal in solution.

[glyoxal]	Time observed	%SOD active
250 μ M	Initial	91.5
	1day	43.4
1mM	Initial	64.4
	1day	17.0
5mM	Initial	20.5
	1day	4.20
25mM	Initial	2.63
	1day	0

3.C. MDHB INHIBITION

My group observed the effect the catechol functionality would have on inhibition of SOD. Observations suggest that the catechol functionality does interact with the SOD active site. The observed fraction of SOD activity in pH 10 fluoride, buffer solution diminished over time upon the introduction of 50 μ M, 1.25mM, 10mM and 20mM MDHB.(Figure.4).

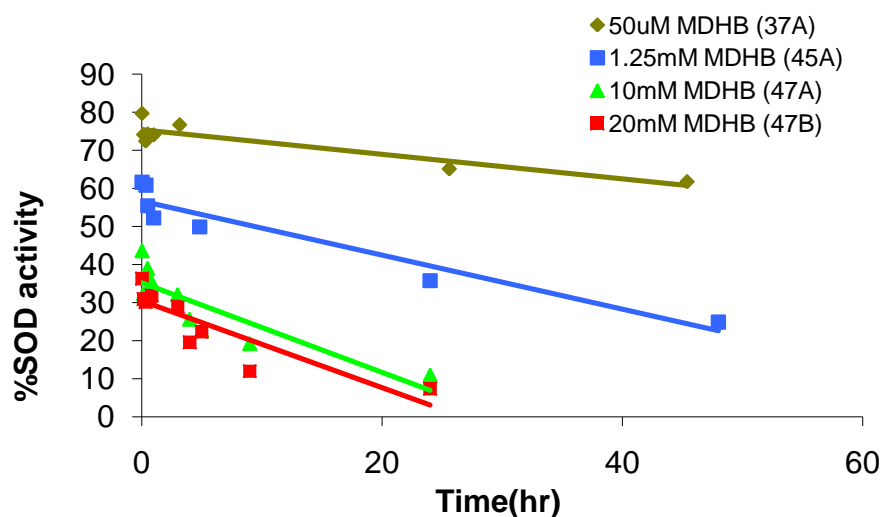


Figure 4: MDHB inhibition of SOD in pH 10 glycine buffer

Observed initial SOD activity however was not 100% at any of the observed concentrations of MDHB. Initial activity was diminished as the concentration of MDHB increased. Upon the addition of MDHB to our pH 10 fluoride, SOD buffer solution a brown color was noticed which indicated oxidation of the inhibitor. We decided not to pursue this further since it was unclear whether inhibitor oxidation affected SOD inhibition.

3.D. QUERCITIN MECHANISM OF INHIBITION

As described in the introduction, compounds that strongly bind copper have been shown to inhibit SOD. Our experiments indicate that quercetin (and presumably other flavonoids as well) does not inhibit SOD by this mechanism. As shown in the two left columns in Figure 5, the fluoride ^{19}F NMR relaxation rate (R_2) is greatly enhanced by SOD, but not by quercetin inhibited SOD.

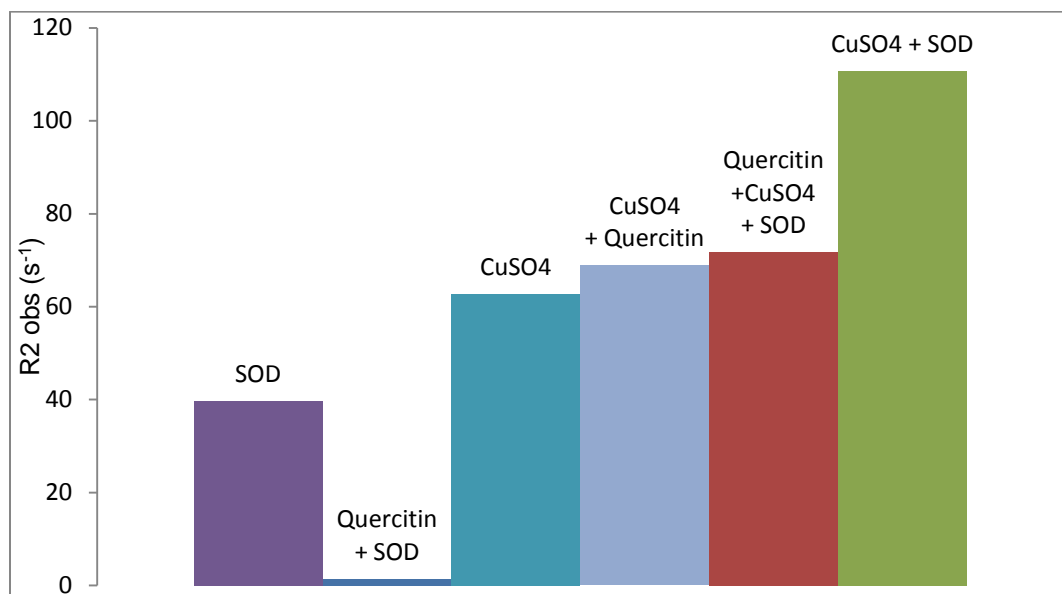


Figure 5: R_2 of fluoride in the presence of CuSO_4 , quercetin and SOD dissolved in pH 10 buffer

200 μM CuSO_4 containing solutions increased the observed fluoride R_2 by about the same amount that 10^{-7} SOD does. Comparing the second two columns indicates that quercetin showed no appreciable effect on Cu^{2+} relaxation of fluoride. Comparing the far right hand column ($\text{CuSO}_4 + \text{SOD}$) to first and third columns from the left (SOD and CuSO_4 , respectively) shows that the relaxation effects of the CuSO_4 and SOD are additive. That is, Cu^{2+} relaxation of fluoride and SOD relaxation of fluoride are independent of each other, and their overall R_2 value equals the sum of their separate R_2 values. Addition of quercetin to the sample containing the CuSO_4 and SOD gave a sample whose relaxation rate (second from right) is similar to that produced by CuSO_4 plus quercetin alone (without the SOD). These observations indicate that Cu^{2+} does not affect the ability of quercetin to inhibit SOD.

3.E. PH DEPENDANT QUERCETIN INHIBITION OF Cu/Zn-SOD

We performed kinetic studies of SOD inhibition by quercetin at pH values ranging from 6.2 to 10.5 (Figures 6 through 14). These studies indicated that inhibition of SOD by quercetin is a two step mechanism. The first step appears to be a rapid equilibrium, giving rise to an initial drop in observed activity. The pH dependence of this step suggests that the inhibitor must be deprotonated in order to bind to SOD active site. The slow inhibition of SOD observed within the pH ranges of 9 to 10.5 is likely the result of the enzyme being deprotonated. Another member of our group has shown evidence that other compounds inactivate SOD by such a mechanism.¹⁴

At pH's 6.16 and 7.01 enzyme activity begins at 100% and drops at a certain rate to around 80% (Figure.6 & Figure.7). At solution pH 7.3 initial enzyme activity drops to ~80% and proceeds to 60% where it reaches equilibrium (Figure.8). At solution pH 8 initial activity was observed to be 35%. Over the course of the experiment enzyme activity then increases reaching equilibrium at ~60% (Figure.9). For solutions at pH's 8.5 (Figure.10), 9.0 (Figure.11) and 9.5 (Figure.12) initial enzyme activity is around 35%. For solution pH 8.5 (Figure.10) enzyme activity then increases from 35% to 40% where it reaches equilibrium. For solution pH 9 (Figure.11) and 9.5 (Figure.12) enzyme activity increases from around 35% to around 40% but then sharply drops approaching full inhibition by the end of our observations. For solutions of pH 10 and 10.5 initial enzyme activity is around 40% where it then decreases until it approaches full inhibition over the course of our experiments.

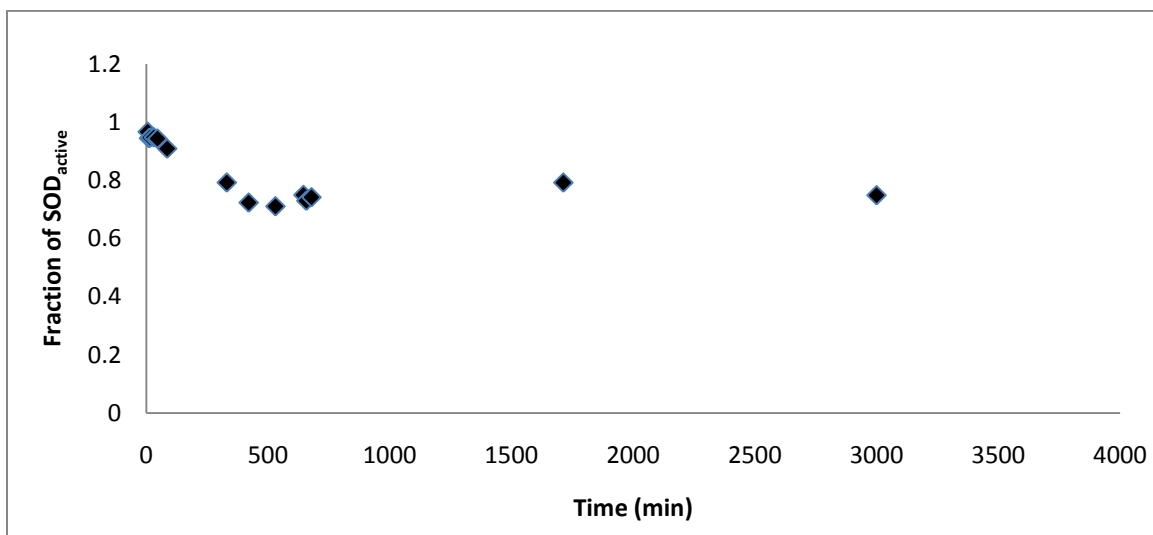


Figure 6: Inhibition of Cu/Zn-SOD by 50 μ M quercetin in pH 6.16 citrate buffer

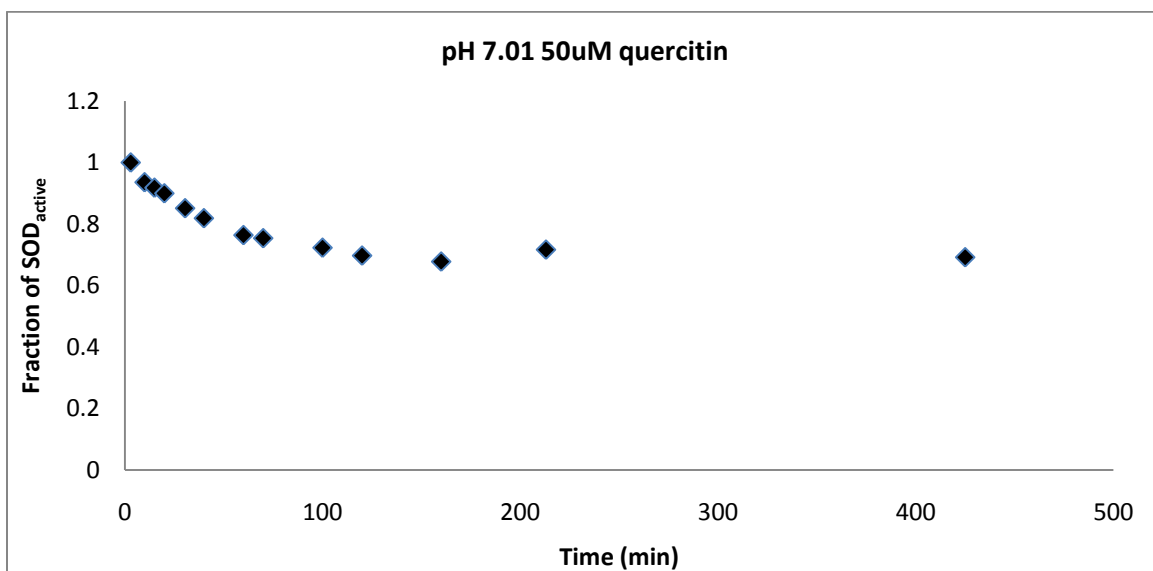


Figure 7: Inhibition of Cu/Zn-SOD by 50 μ M quercetin dissolved in pH 7.01 HEPES buffer

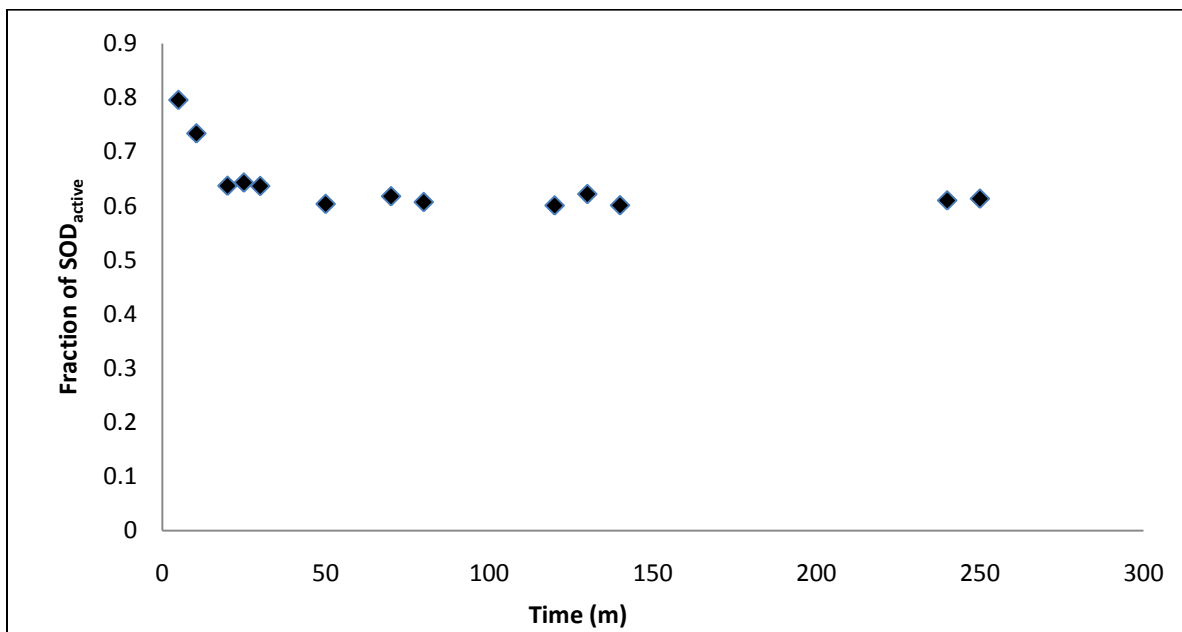


Figure 8: Inhibition of Cu/Zn-SOD by 50 μ M quercetin dissolved in pH 7.3 HEPES buffer

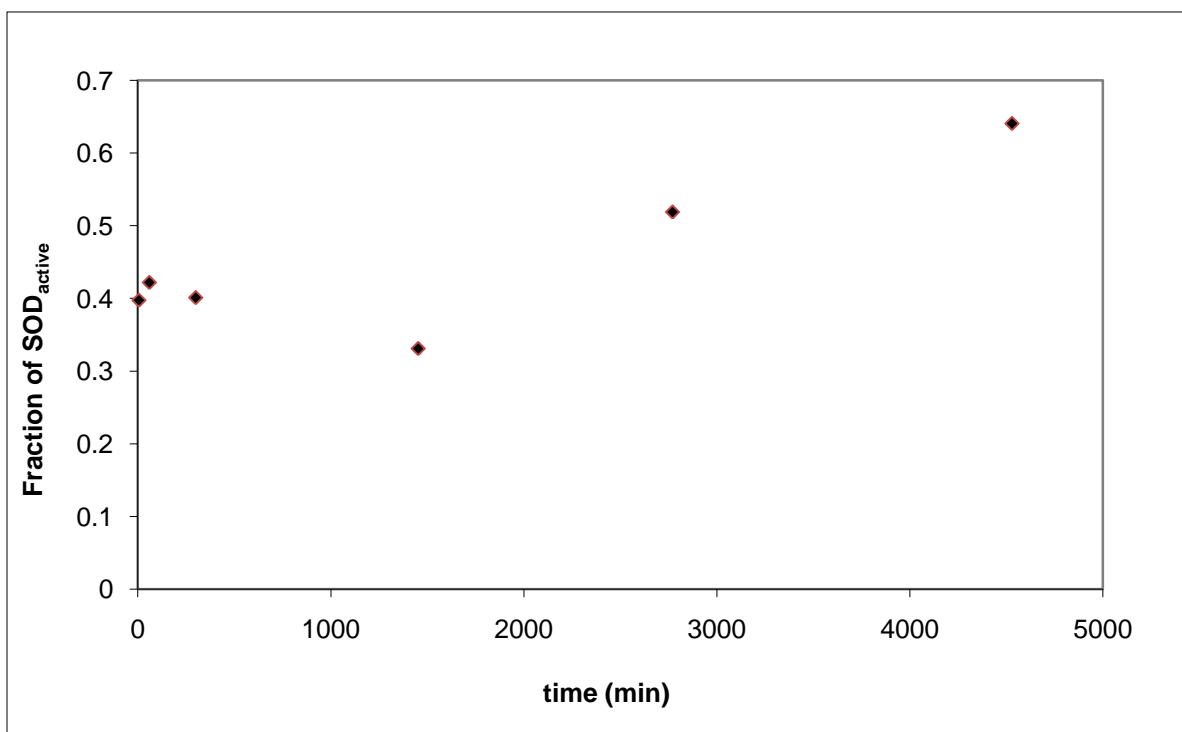


Figure 9: Inhibition of Cu/ZN-SOD by 50 μ M quercetin dissolved in pH 8.0 TRIS buffer

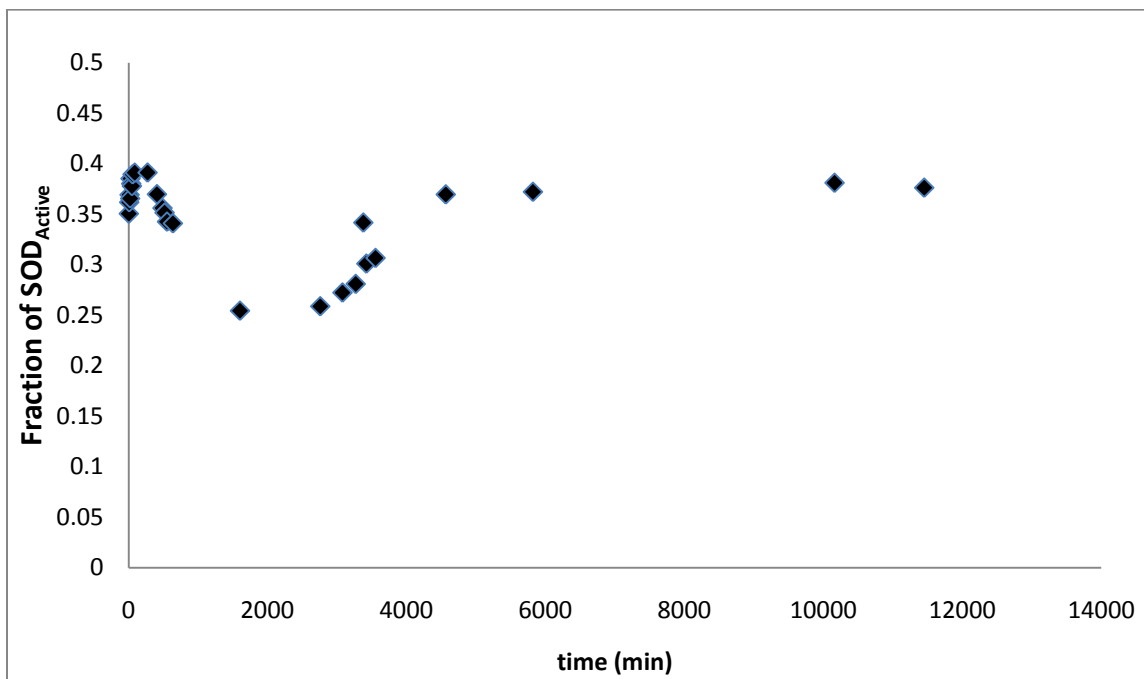


Figure 10: Inhibition of Cu/Zn-SOD by 50µM quercetin dissolved in pH 8.5 TRIS buffer

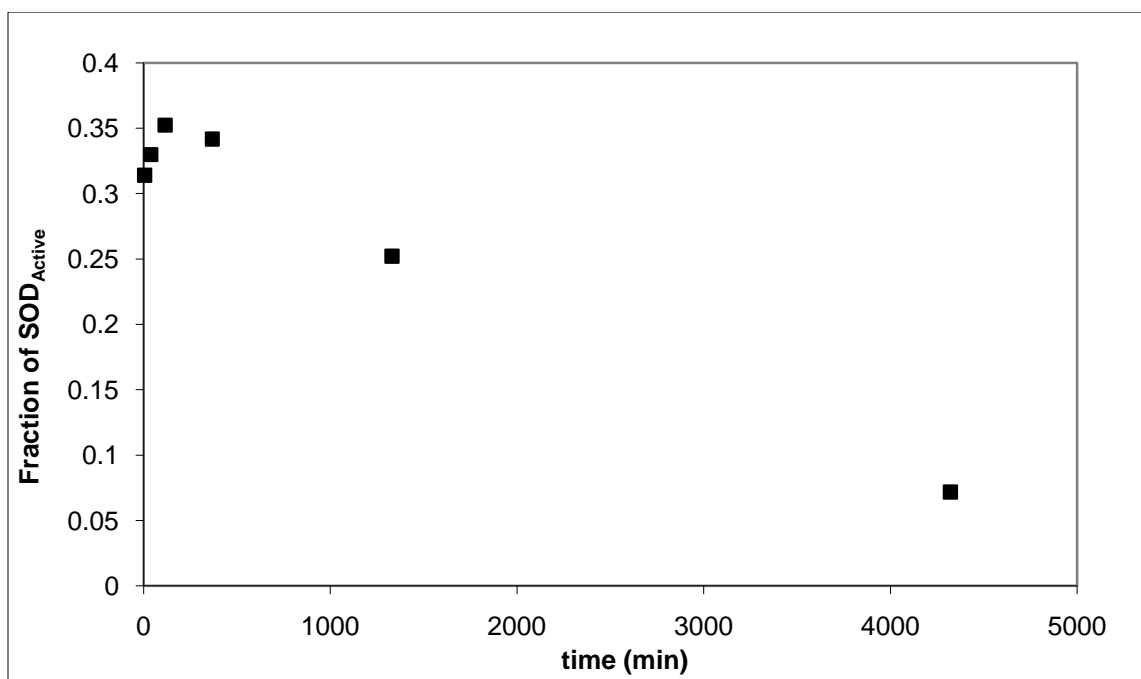


Figure 11: Inhibition of Cu/ZN-SOD by 50µM quercetin dissolved in pH 9 glycine buffer

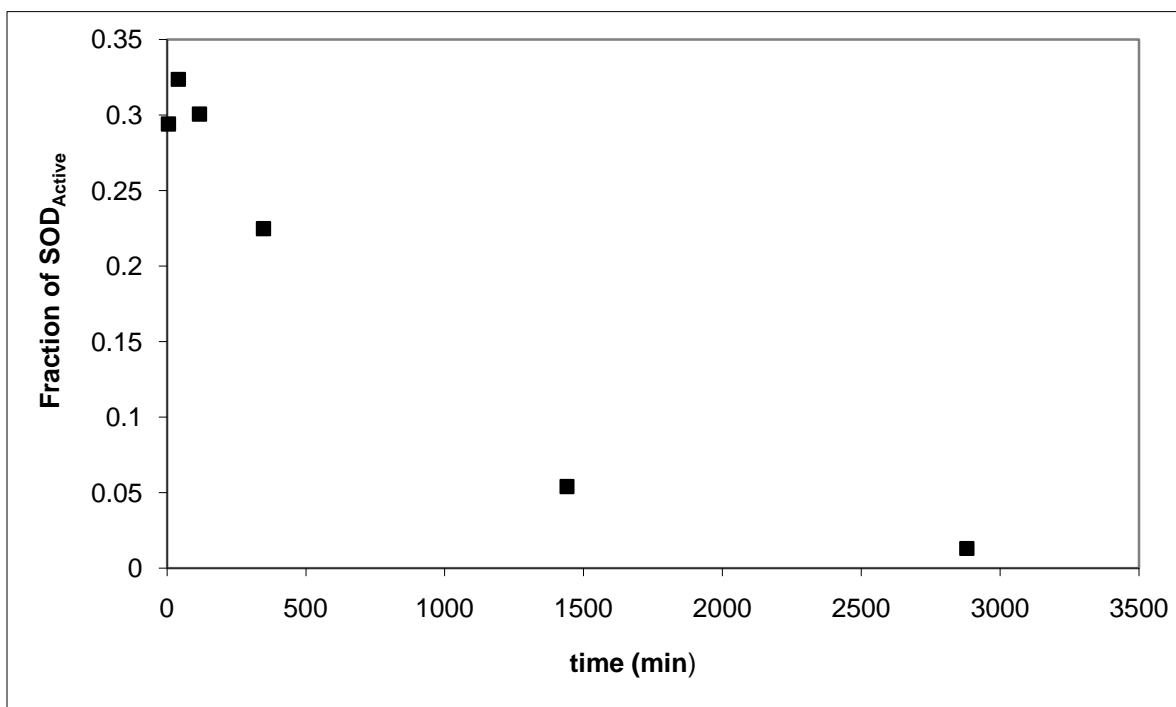


Figure 12: Inhibition of Cu/Zn-SOD by 50 μ M quercetin dissolved in pH 9.5 glycine buffer

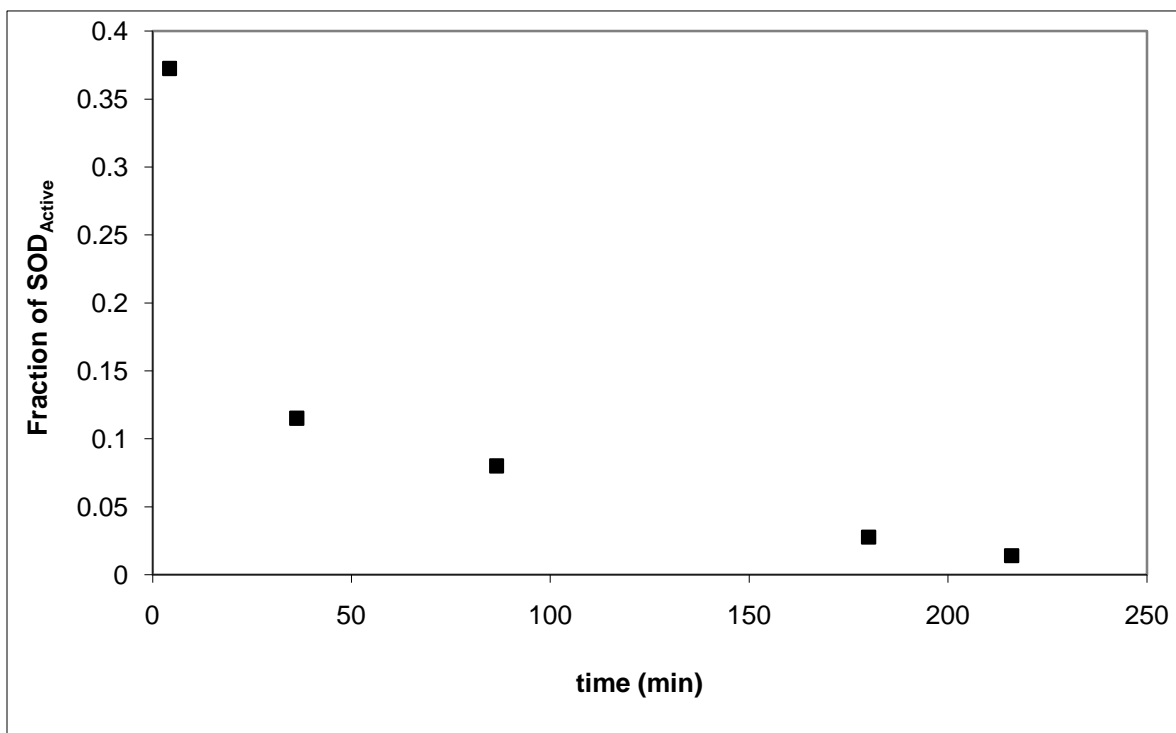


Figure 13: Inhibition of Cu/Zn-SOD by 50 μ M quercetin dissolved in pH 9.98 glycine buffer

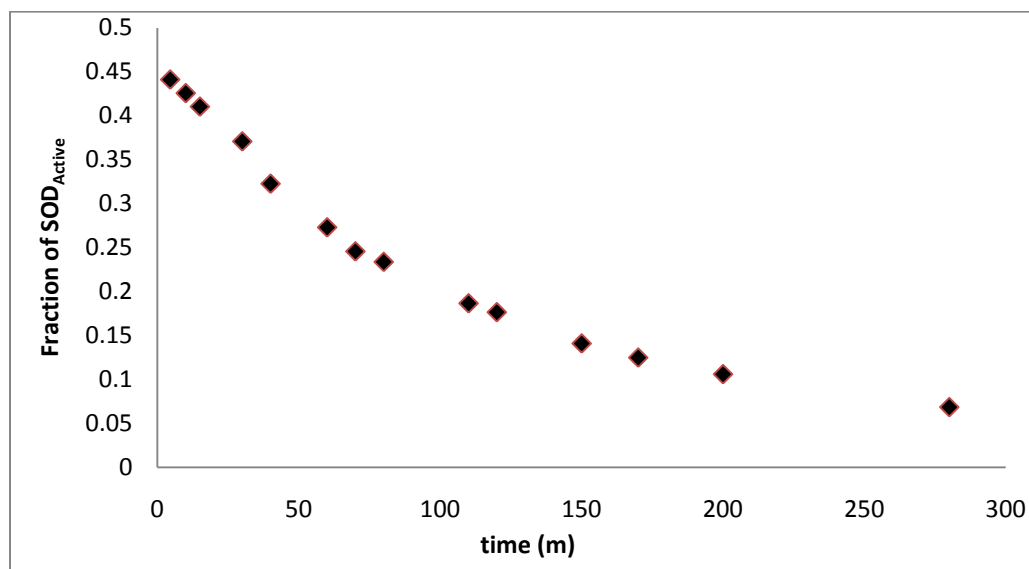


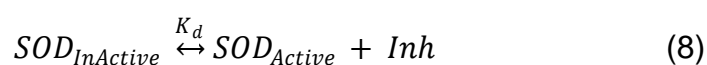
Figure 14: Inhibition of Cu/Zn-SOD by 50 μ M quercetin dissolved in pH 10.5 glycine buffer

3.F.1 DISSOCIATION CONSTANTS FOR FLAVONOID INHIBITORS OF SOD

Our group has observed inhibition of SOD by morin, fisitin, quercetin, taxifolin, kaempferol, luteolin and methoxyquercetin. Plots of flavonoid dissociation constants (K_d) and Dimerization constants (K_{dimer}) were calculated and are represented in Table 4.

Table 4: Calculated Cu/Zn-SOD inhibitor K_d accounting for dimerization		
Flavone	K_d (μ M)	K_{dimer} (μ M ⁻¹)
luteolin	480	0.000009
morin	397	0.0009
quercetin	< 6	>0.281
methoxyquercetin	inconclusive	inconclusive
taxifolin	80-110	0.010 to 0.0034
kaempferol	~30	0.73
fisitin	10-30	0.15 to 0.011

No inhibition of SOD was observed for galangin and 3,3-dihydroxyflavone within the concentration range of 6.25 μ M and 400 μ M. The proposed mechanism for inhibition of SOD by flavonoids is represented in (Equation.8). The fraction of SOD inactive ($SOD_{Inactive}$) plus bound inhibitor is the reactant at equilibrium. The fraction of SOD active (SOD_{Active}) and free inhibitor (Inh) are the products in equilibrium.



Inhibition of SOD active site is most likely achieved by one molecule of inhibitor due to the active site's narrow channel and small active site. Using this equilibrium expression the dissociation constant ($K_{d,inhibitor}$) can be solved using the equation

$$K_d = \frac{SOD_{Active} [Inh]}{SOD_{Inactive}} \quad (9A)$$

Since the fraction of SOD active (SOD_{Active}) plus the fraction of SOD inactive ($SOD_{inactive}$) must equal 1 and the equilibrium expression can be rewritten.

$$\frac{1}{SOD_{Active}} - 1 = \frac{[Inh]}{K_d} \quad (9B)$$

Equation 8B predicts that plots of $\{(1/SOD_{Active}) - 1\}$ versus $[Inh]$ should be linear with a slope equal to $1/K_d$. As shown in Figures 15 through 21, however, these plots show pronounced curvature. We have observed precipitation of

flavonoid inhibitors in aqueous buffer solution, and we propose that the curvature in Figures 15 through 21 may be due to dimerization or other aggregation of the inhibitors. Smith et al. reported that inhibitors dimerize, trimerize and further aggregate within the concentration range that I observed the fraction of SOD activity.¹³ If the dimerization constants were known, the concentration of monomeric inhibitor could be calculated using the quadratic below.

$$.Inh_{mono} = \frac{-1 + \sqrt{1 - 8(K_{dimer})(-[Inh])}}{4(K_{dimer})} \quad (10)$$

Values of K_{dimer} and K_d were estimated by fitting a curve predicted by equations 10 and 9B to the data. Calculated values of $1/SOD_{Active} - 1$ were calculated by changing values for K_{dimer} and K_d to minimize the sum of the total differences between the calculated and observed values. Final calculated values are represented by the dashed lines in Figures 15 through 21.

We observed a decrease in initial SOD activity (A_0) at increasing concentrations of morin, quercetin, taxifolin, fisitin, luteolin, kaempferol and methoxyquercetin in pH 8.01 fluoride, TRIS, SOD buffer solution.

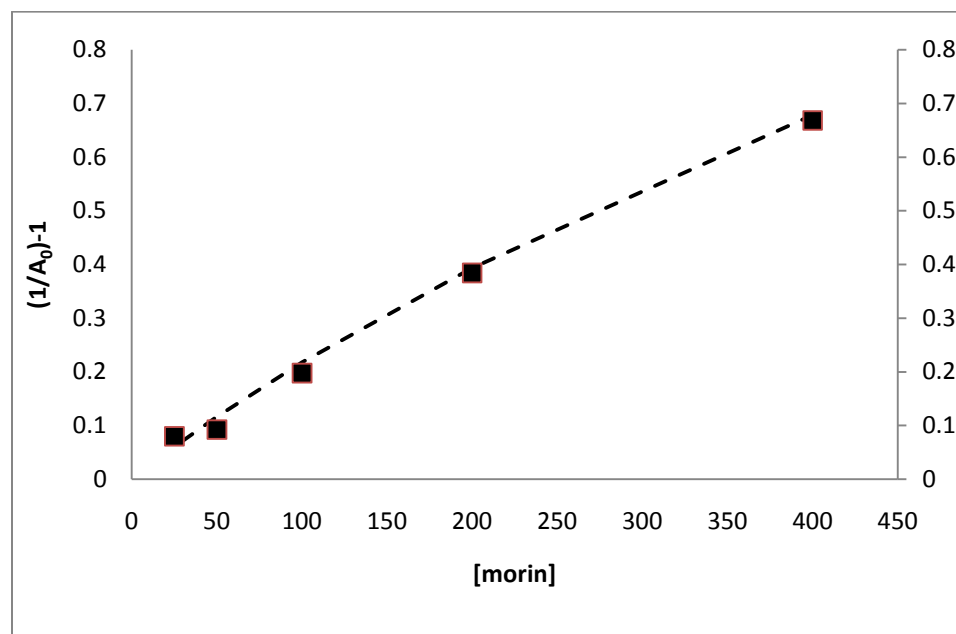


Figure 15: Initial inhibition of Cu/Zn-SOD by morin dissolved in pH 8.01 TRIS buffer.
Observed $(1/A_0)-1$ ■ ; calculated $(1/A_0)-1$ -----

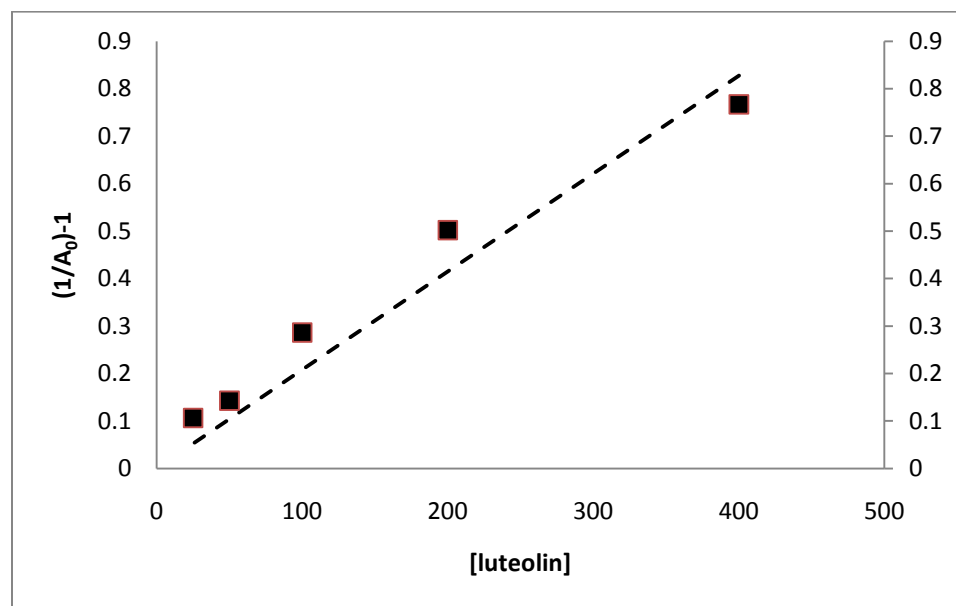


Figure 16: Initial inhibition of Cu/Zn-SOD by luteolin dissolved in pH 8.01 TRIS buffer.
Observed $(1/A_0)-1$ ■ ; calculated $(1/A_0)-1$ -----

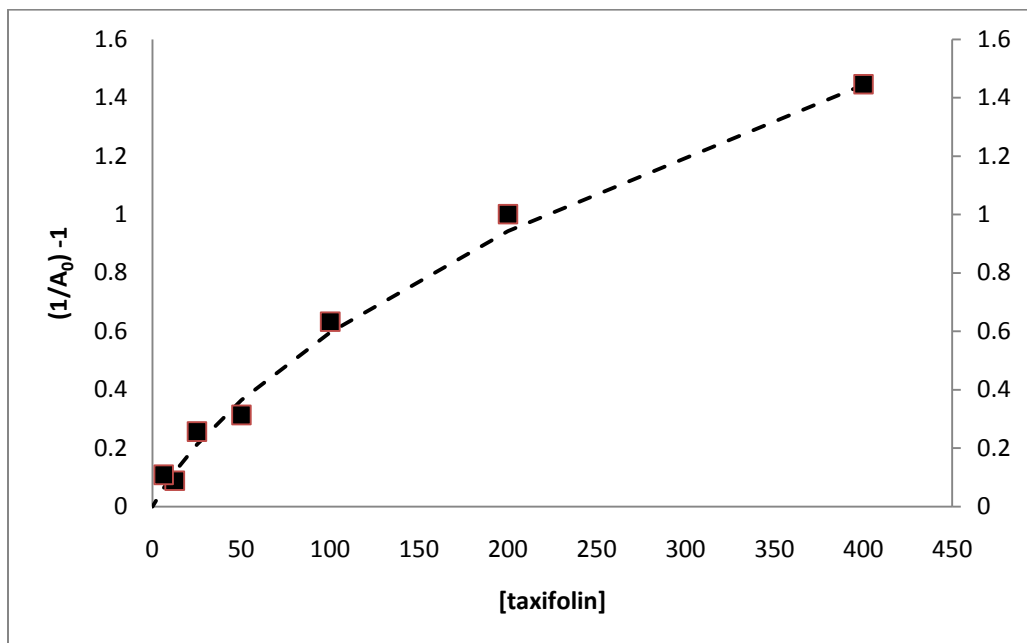


Figure 17: Initial inhibition of Cu/Zn-SOD by taxifolin dissolved in pH 8.01 TRIS buffer.
Observed $(1/A_0)^{-1}$ ■ ; calculated $(1/A_0)^{-1}$ -----

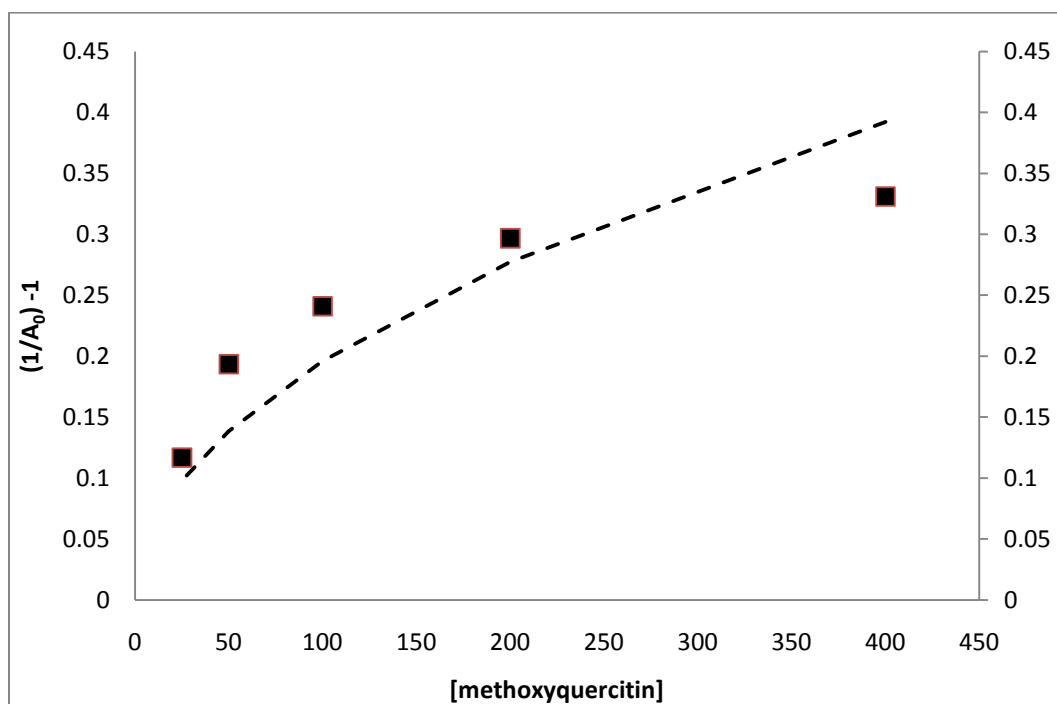


Figure 18: Initial inhibition of Cu/Zn-SOD by methoxyquercetin dissolved in pH 8.01 TRIS buffer.
Observed $(1/A_0)^{-1}$ ■ ; calculated $(1/A_0)^{-1}$ -----

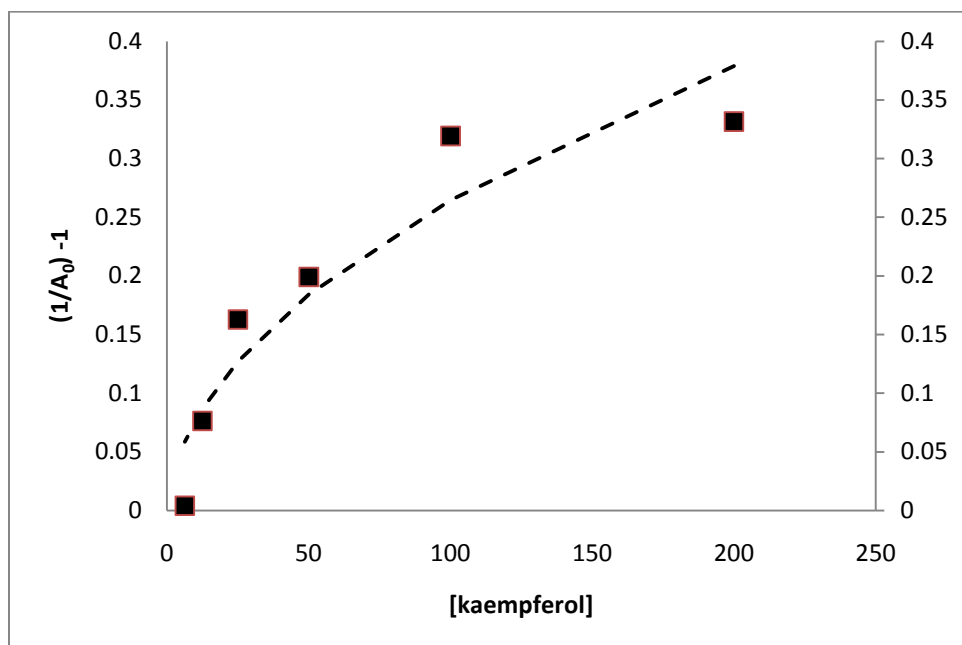


Figure 19: Initial inhibition of Cu/Zn-SOD by kaempferol dissolved in pH 8.01 TRIS buffer.
Observed (1/A₀)⁻¹ ■ ; calculated (1/A₀)⁻¹ -----

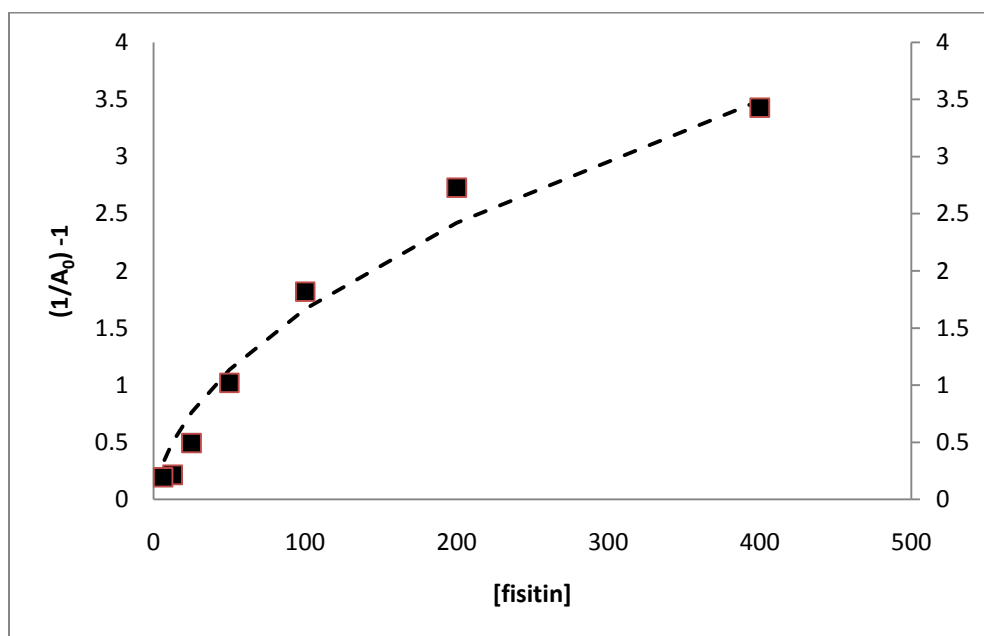


Figure 20: Initial inhibition of Cu/Zn-SOD by fisitin dissolved in pH 8.01 TRIS buffer.
Observed (1/A₀)⁻¹ ■ ; calculated (1/A₀)⁻¹ -----

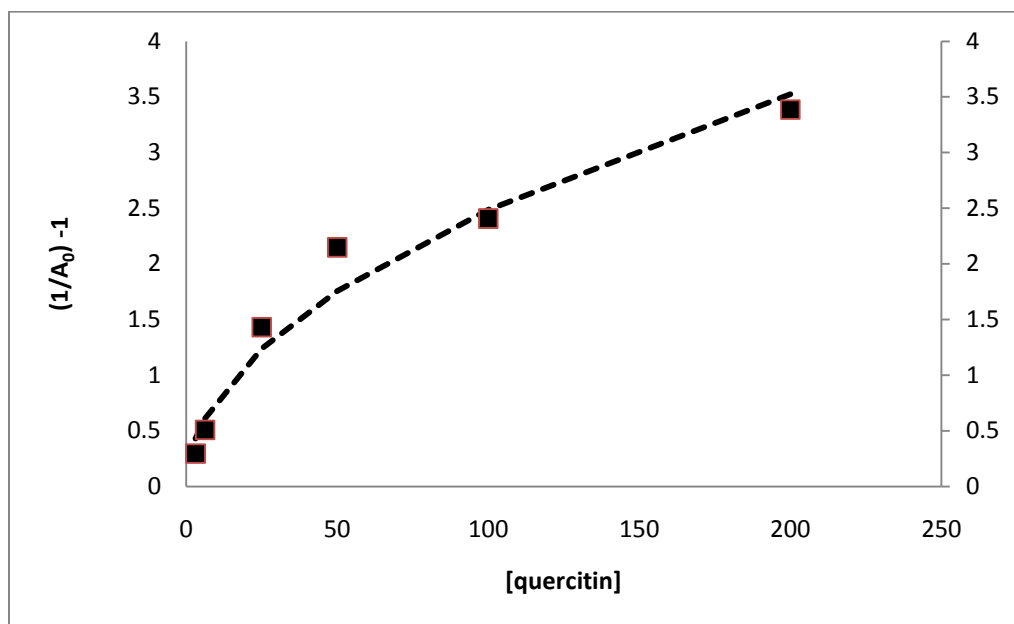


Figure 21: Initial inhibition of Cu/Zn-SOD by quercetin dissolved in pH 8.01 TRIS buffer. Observed $(1/A_0)^{-1}$ ■ ; calculated $(1/A_0)^{-1}$ -----

Plots for morin, and luteolin show a relatively linear correlation suggesting little or no dimerization of inhibitor at these concentrations. Similar plots for taxifolin, quercetin, kaempferol, fisitin and methoxyquercetin have shown significant curvature within the observed concentration range of 6.25 μ M -400 μ M suggesting dimerization of inhibitor (Figures 17-21). The sum of the differences for methoxyquercetin plots were minimized for K_d values below 10 μ M. The calculated K_d plot for methoxyquercetin does not fit the observed plot and the amount of inhibition observed does not agree with the calculated K_d range for methoxyquercetin (Figure.18).

3.F.2 DIMERIZATION OF FLAVONOID INHIBITORS

Dimerization of flavonoids was investigated by luminescence spectroscopy. Spectra for the flavonoids quercetin, morin, kaempferol, fisitin and taxifolin show observable peaks within between 300nm and 460nm.

Inhibitor:	Excitation peaks:	Emission peaks:
quercetin	415nm, 440nm	490nm, 515nm
morin	390nm, 440nm	515nm, 550nm
taxifolin	410nm, 440nm	480nm, 515nm
fisitin	330nm, 385nm	490nm, 515nm
kaempferol	405nm, 435nm	475nm, 500nm

Smith et al. proposed that shorter wavelengths to longer wavelengths indicate dimerization of flavonoids such as quercetin and kaempferol.¹³ It is apparent from our results that the peaks at shorter wavelengths are diminishing in relation to the peaks at longer wavelengths for all observed flavones (Figures 22,23,24,25,26). The peak shift for all observed flavonoids could be the explanation for the curvature of K_d plots previously observed by our group if the monomer is the form of inhibitor that binds to enzyme active site.

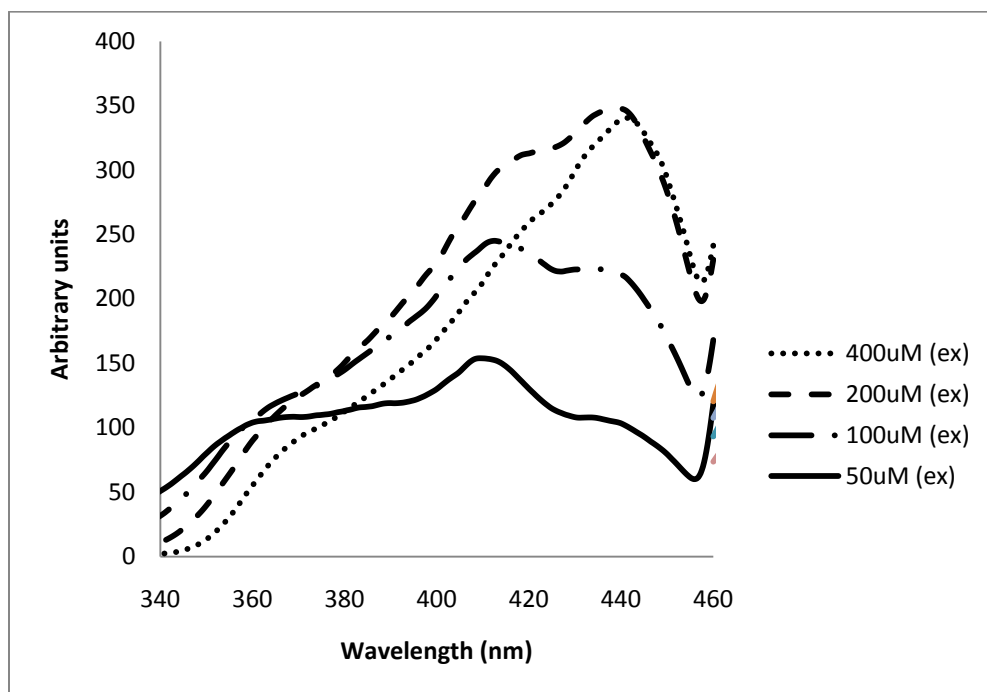


Figure 22: Absorbance spectra for taxifolin dissolved in 8.01 fluoride TRIS soln.

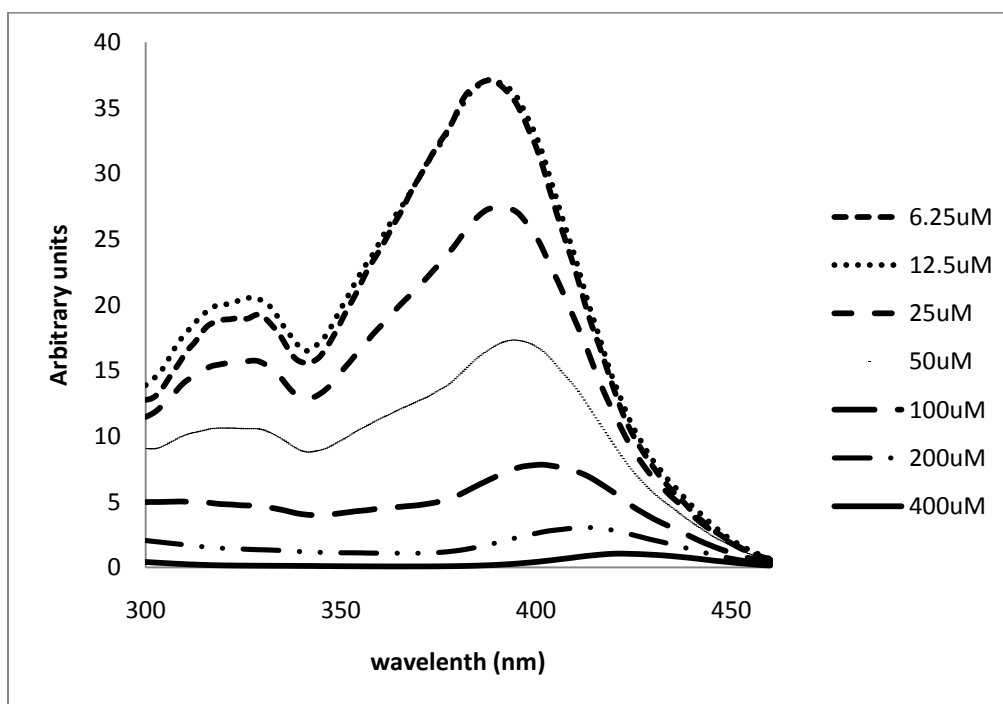


Figure 23: Absorbance spectra for fisitin dissolved in 8.01 fluoride TRIS soln.

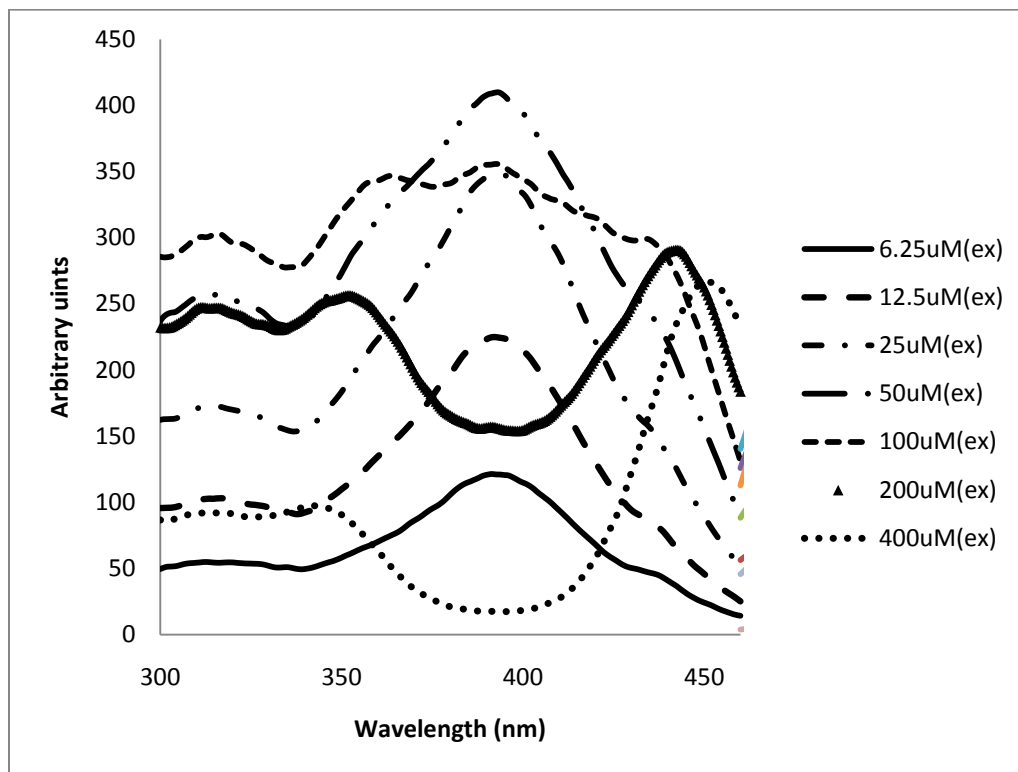


Figure 24: Absorbance spectra for morin dissolved in 8.01 fluoride TRIS soln.

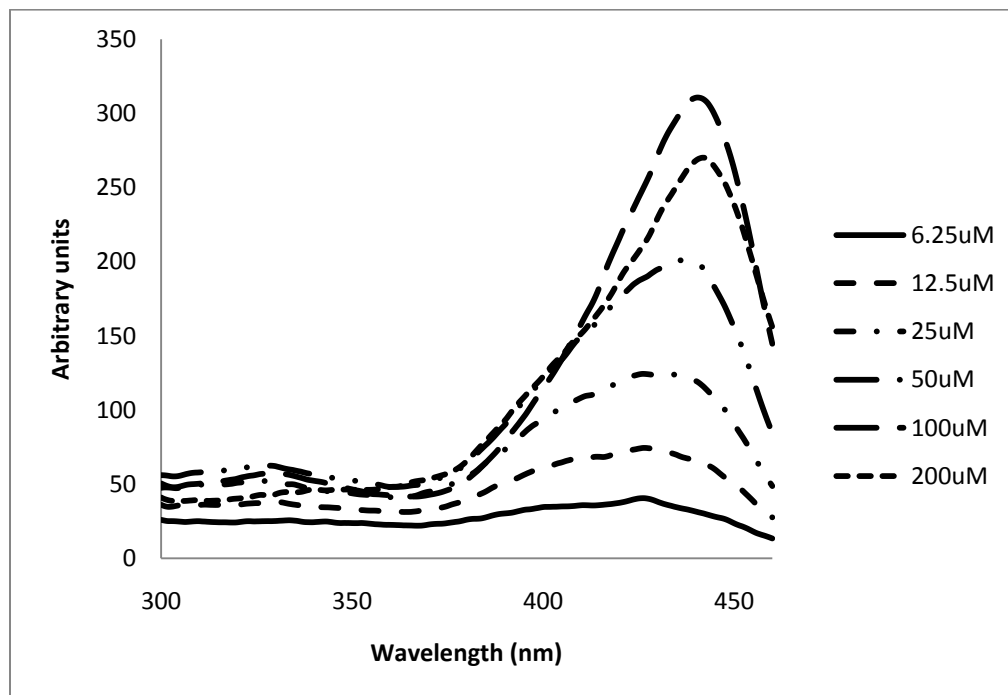


Figure 25: Absorbance spectra for kaempferol dissolved in 8.01 fluoride TRIS soln.

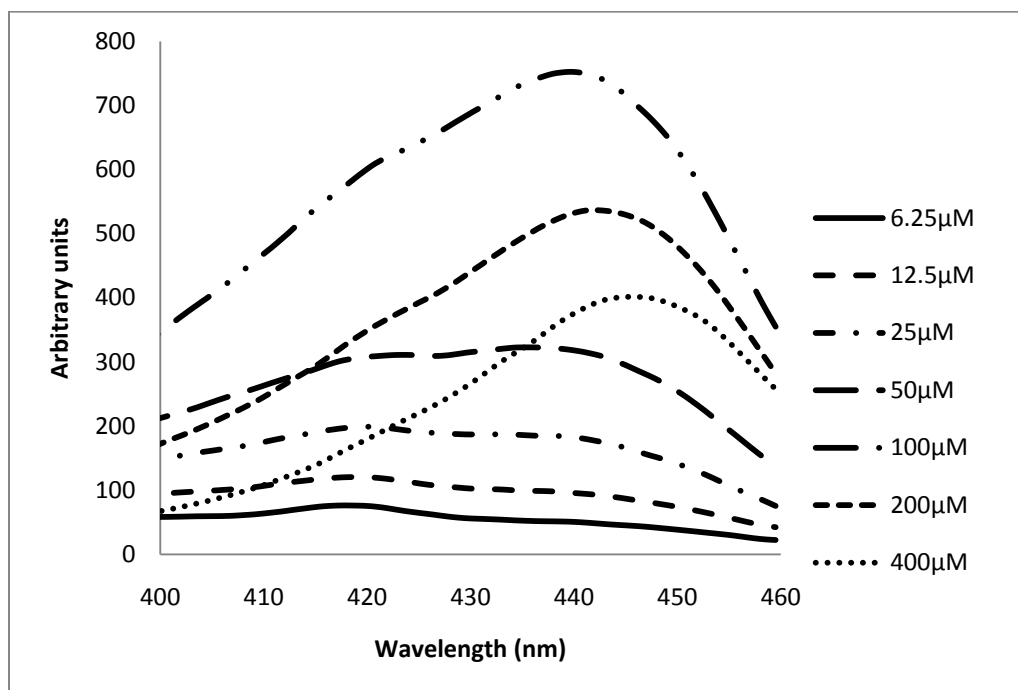


Figure 26: Absorbance spectra for quercetin dissolved in 8.01 fluoride TRIS soln.

4. CONCLUSIONS

The small molecules glyoxal, MDHB and DDC have shown significant inhibition of SOD activity. Though these molecules are good inhibitors their use for inhibition *In vivo* is impossible due to their toxicity. The observed inhibition of SOD by these small molecules has aided our group in selecting potential inhibitors for further assays for SOD inhibition.

Our observed reaction order values disagree with this mechanism and indicate that the first step of DDC binding to SOD active site must be rate limiting.

Observed plots of SOD activity suggest that MDHB inhibition in pH 10 solution is a two step mechanism with the first being fast and a result of our inhibitor inactivating SOD. The second slower step that proceeds toward full enzyme inactivation is most likely the result of enzyme deprotonation.¹⁴ A dissociation constant for MDHB cannot be accurately calculated due to observed oxidation of this inhibitor in aqueous fluoride buffer solution. Further experiments which prevent this oxidation are required before an accurate dissociation constant can be calculated.

2-ME and ENMD-1198 have shown no observed inhibition of SOD in the pH 10 solution that I observed. Another member of my group has shown that 2-ME does inhibit SOD at pH 10 with carbonate added to the solution.¹⁰

The ability of quercetin to inhibit SOD in the presence of CuSO_4 indicates that quercetin does not sequester the metal from SOD active site. If quercetin sequestered the Cu from the SOD active site then the presence of an excess of Cu^{2+} in solution would prevent inhibition by binding to quercetin preventing the loss of SOD activity. Based on our observations quercetin and other flavonoids bind at or near SOD active site.

Based on the observed dissociation constants it appears that the 3-hydroxyl is important for inhibitor binding to SOD. This is shown by the change in K_d between quercetin ($K_d < 7\mu\text{M}$) and luteolin ($K_d = 480\mu\text{M}$) where luteolin only differs from quercetin by the absence of the 3-hydroxyl. The site at which the enzyme is deprotonated has also shown an effect on the dissociation constant. Flavonoids that are deprotonated at the 7-hydroxyl such as quercetin, fisetin and kaempferol have a higher affinity to bind to enzyme than those that are deprotonated at the 2'-hydroxyl such as morin.

REFERENCES

-
- ¹ Ewing, James F.; Janero, David R. Microplate Superoxide Dismutase Assay Employing a Nonenzymatic Superoxide Generator. *Analytical Biochemistry*. **1995**, 232, 243-248
- ² Huang, Peng; Feng, Li; Oldham, Elizabeth A.; Keating, Michael J.; Plunkett, William Superoxide dismutase as a target for the selective killing of cancer cells, *Nature* **2000**, 407, 390-395
- ³ Soulère, Laurent; Viodé, Cécile; Périé, Jacques; Hoffmann, Pascal Selective Inhibition of Fe- versus Cu/Zn-Superoxide Dismutases by 2,3-Dihydroxybenzoic Acid Derivatives, *Chem. Pharm. Bull.* **2002**, 50(5), 578-582
- ⁴ Bertini, Ivano; Mangani, Stefano; Viezzoli, Maria S. Structure and Properties of Copper-Zinc Superoxide Dismutases. *Advances in Inorganic Chemistry Vol 45*. **1998**, 127-250
- ⁵ Rigo, Adelio; Viglino, Paolo; Argese, Emanuele; Terenzi, Mario; Rotilio, Giuseppe Nuclear magnetic Relaxation of ¹⁹F as a Novel Assay method of Superoxide Dismutase, *The Journal of Biological Chemistry* **1979**, 254, No. 6, 1759-1760
- ⁶ Heikilla, Richard E.; Cabbat Felicitas S.; Cohen Gerald In Vivo Inhibition of Superoxide Dismutase in Mice by Diethyldithiocarbamate. *J. Biological Chemistry*. **1976**, 7, 2182-2185
- ⁷ Soulère, Laurent; Delplace, Patrick; Davioud-Charvet, Elisabeth; Py, Sandrine; Sergheraert, Christian; Périé, Jacques; Ricard, Isabelle; Hoffmann, Pascal; Dive, Daniel Screening of *Plasmodium falciparum* Iron Superoxide Dismutase Inhibitors and Accuracy of the SOD-Assays. *Bioorganic & Medicinal Chemistry* **2003**, 11, 4941-4944
- ⁸ Lakhani, Nehal J.; Sarkar, Mohamadi A.; Venitz, Jurgen; Figg, William D. 2-Methoxyestradiol, a Promising Anticancer Agent, *WebMD [Online]* **2003**, 23(2) <http://www.medscape.com/viewarticle/449725> (accessed March 21st 2010)
- ⁹ <http://www.nutritional-supplement-guides.com/Quercitin.html> **2006-2007**

-
- ¹⁰ Experiments by Michelle Yost on the inhibition of SOD by 2-ME and the integrated tfa resonance signal
- ¹¹ Musialik, Malgorzat; Kuzmicz, Rafal; Pawlowski, Tomasz S.; Litwinienko, Grzegorz Acidity of Hydroxyl Groups: An Overlooked influence on Antiradical Properties of Flavonoids. *J.Org.Chem.* [Online] **2009**, 74, 2699-2709 <http://pubs.acs.org> (accessed October 15th 2009).
- ¹² Herrero-Martínez, José M.: Sanmartin, Meritxell; Rosés Martí; Bosch, Elisabeth; Ràfols, Clara Determination of dissociation constants of flavonoids by capillary electrophoresis. *Electrophoresis*. **2005**, 26, 1886-1895
- ¹³ Smith, Gerald Markham, Kenneth ;Tautomerism of Flavonol Glucosides Journal of Photochemistry and Photobiology A: Chemistry 118, New Zealand Institute for industrial Research and Development June **1998** pg. 99-105
- ¹⁴ Experiments by Megan Arrington with 9-anthracinecarboxylic acid